Surface Micellization Patterns of Quaternary Ammonium Surfactants on Mica

Heather N. Patrick,[†,‡] Gregory G. Warr,*[,†,§] Srinivas Manne,[||] and Ilhan A. Aksay[‡]

School of Chemistry, University of Sydney, Sydney, New South Wales, 2006 Australia, Princeton Materials Institute, Princeton University, Princeton, New Jersey 08544, Rhone-Poulenc/CNRS Complex Fluids Laboratory, Cranbury, New Jersey 08512, and Department of Physics, University of Arizona, Tucson, Arizona 85721

Received November 17, 1998

The microscopic equilibrium structures of adsorbed films of quaternary ammonium surfactants on mica have been investigated by noncontact atomic force microscopy imaging as a function of alkyl chain length and headgroup structure. Spherical and cylindrical surface micelles were observed; these were found to be related to bulk solution self-assembly and the surfactant packing parameter, v/a_0l_c. Shape transitions in the surface aggregates were observed on changing the counterion between chloride, bromide, and salicylate.

Introduction

To understand observable properties of adsorbed films of surface-active agents on solids, we require an understanding of the microscopic nature of these interfaces. The first proposal of surface hemimicelles was in 1955;[1] since then the structure of adsorbed films of surfactants on solid surfaces has been investigated by many techniques. Direct evidence of surface micelles was gleaned principally from fluorescence probe studies,[2] although other techniques also give similar indications.[3]

The atomic force microscope (AFM) used in a noncontact mode in solution[4−10] has recently been applied to equilibrium adsorbed surfactant films. Images of adsorbed films from this technique show aggregates which bear remarkable similarities to solution self-assembly structures; images have been interpreted as showing the adsorbed layer to consist of full spheres,[6,10] flexible cylinders,[6,10] and bilayers[6,10] on hydrophilic substrates, and rigid hemicylinders on graphite.[5−7]

In the case of nonionic poly(oxyethylene) surfactants adsorbed on graphite, adsorbed structures were found to be related to the bulk self-assembled geometries of the amphiphiles in water.[11] Similarly, a hemicylinder to flat sheet adsorbed film structure has been reported upon the addition of dodecanol to sodium dodecyl sulfate films on graphite, which parallels the bulk phase transition.[12] However the influence of graphite on the adsorbed layer structure is so strong that solution equilibria can be overwhelmed. For example, hemispheres have never been reported on graphite.

Mica is a model hydrophilic surface and has been previously used to study interaction forces in solution. These include measurements of electrical double layer forces between two adsorbed cationic surfactant films.[13] There are obvious implications on the interpretation of these force measurements if the layers were composed of surface aggregates or micelles rather than the supposed laterally homogeneous bilayers.

In this work we investigate the equilibrium adsorbed layer structures of a variety of cationic surfactants on the hydrophilic, negatively charged substrate mica by AFM imaging. The solution behavior and phase equilibria of surfactants of the type alkyl trimethyl, triethyl, tripropyl, and tributyl quaternary ammonium bromides (abbreviated as $C_{12-16}NMe_3$, Et_3, Pr_3, Bu_3Br) show systematic variations with molecular structure and hence shape.[14,15] Alterations in the headgroup size, alkyl tail length, and the counterion all affect solution self-assembly. It is our hypothesis that these changes will also be reflected in the structure of adsorbed films on mica.

Experimental Section

The surfactants used were a set of quaternary ammonium bromides with varying alkyl tail lengths and headgroup sizes. $C_{12}NMe_3Br$ (DTAB) and $C_{14}NMe_3Br$ (TTAB) were purchased from Fluka. Other bromide surfactants were prepared by the reaction

* To whom correspondence should be addressed at the University of Sydney. E-mail: g.warr@chem.usyd.edu.au.
† University of Sydney.
‡ Princeton University.
§ Rhone-Poulenc/CNRS Complex Fluids Laboratory.
|| University of Arizona.

(1) Gaudin, A. M.; Fuerstenau, D. W. *Trans. AIME* **1955**, *202*, 958−962.
(2) (a) Levitz, P.; El Meri, A.; Keravis, D.; Van Damme, H. *J. Colloid Interface Sci.* **1984**, *99*, 484−492. (b) Levitz, P.; Van Damme, H.; Keravis, D. *J. Phys. Chem.* **1984**, *88*, 2228−2235. (c) Levitz, P.; Van Damme, H. *J. Phys. Chem.* **1986**, *90*, 1302−1310.
(3) Tiberg, F. *J. Chem. Soc., Faraday Trans.* **1996**, *92*, 531−538.
(4) Senden, T. J.; Drummond, C. J.; Kékicheff, P. *Langmuir* **1994**, *10*, 358−362.
(5) Manne, S.; Cleveland, J. P.; Gaub, H. E.; Stucky, G. D.; Hansma, P. K. *Langmuir* **1994**, *10*, 4409−4413.
(6) Manne, S.; Gaub, H. E. *Science* **1995**, *270*, 1480−1482.
(7) Wanless, E. J.; Ducker, W. A. *J. Phys. Chem.* **1996**, *100*, 3207−3214.
(8) Ducker, W. A.; Grant, L. M. *J. Phys. Chem.* **1996**, *100*, 11507−11511.
(9) Jaschke, M.; Butt, H.-J.; Gaub, H. E.; Manne, S. *Langmuir* **1997**, *13*, 1381−1384.
(10) Manne, S.; Schaffer, T. E.; Huo, Q.; Hansma, P. K.; Morse, D. E.; Stucky, G. D.; Aksay, I. A. *Langmuir* **1997**, *13*, 6382−6387.
(11) Patrick, H. N.; Warr, G. G.; Manne, S.; Aksay, I. A. *Langmuir* **1997**, *13*, 4349−4356.
(12) Wanless, E. J.; Davey, T. W.; Ducker, W. A. *Langmuir* **1997**, *13*, 4223−4228.
(13) Pashley, R. M.; Israelachvili, J. N. *Colloids Surf.* **1981**, *2*, 169−187.
(14) Blackmore, E. S.; Tiddy, G. J. T. *J. Chem. Soc., Faraday Trans. 2* **1988**, *84*, 1115−1127.
(15) Buckingham, S. A.; Garvey, C. J.; Warr, G. G. *J. Phys. Chem.* **1993**, *97*, 10236−10244.

10.1021/la981612o CCC: $18.00
Published on Web 02/09/1999

of a 1-bromoalkane with the appropriate trialkylamine followed by multiple recrystallizations, following the procedure described elsewhere.[15] $C_{16}NMe_3Br$ was insoluble at the temperature of the experiment (20 °C) and therefore not examined. The chloride salt of the alkyltrimethylammonium surfactant $C_{12}NMe_3Br$ (DTAC, Tokyo Kasei) was used as received. $C_{14}NMe_3Cl$ (TTAC) was prepared by ion exchange from TTAB. Due to its high binding efficiency, sodium salicylate (Fluka) was added directly to the appropriate bromide surfactant solutions.

Atomic force microscopy was performed using a Digital Instruments Nanoscope III in contact mode. The imaging method was to use the double layer repulsion between the tip and the surface layer and fly the tip over the adsorbed film.[5] The mica substrate was freshly cleaved before use with adhesive tape. Silicon nitride cantilevers with nominal spring constants of 0.3 N m^{-1} (DI) were cleaned by UV irradiation for 40 min prior to use. All surfactants were studied at concentrations greater than the critical micelle concentration (cmc), and usually twice the cmc. Surfactant solutions were injected into the liquid cell and thermally equilibrated for about 1 h before imaging. Scan rates were varied between 5 and 14 Hz.

An excess of sodium salicylate (Fluka) solution (~2 M) was added to some solutions. The liquid cell was then flushed with more surfactant solution until a double layer repulsion was once more observed in the force profile; the film was then imaged as previously. This leaves an excess of salicylate which effectively transforms quaternary ammonium surfactant micelles from spheres into cylinders.

Results and Discussion

Force Curves. Force profiles were obtained for each solution after injection into the AFM liquid cell. Figure 1 shows typical force curves for hexadecyltrialkylammonium bromide surfactants on mica. All surfactants studied exhibited similar force profiles, which are consistent with previous studies of ionic surfactants by AFM.[5−7] At large separations between the tip and surface, the tip experiences no force. On the approach of the tip toward the surface, there is an electrostatic double layer repulsion until a point where there is a jump to closer contact: this corresponds to a breakthrough in the adsorbed surfactant layer between the tip and mica. At this point the tip is in contact with mica and its lattice may be imaged. With the force on the tip set to less than the breakthrough force, an image of the adsorbed film may be taken without physical contact between the tip and surface layer. All the figures shown were imaged using this repulsive electrostatic force between the tip and sample.

Adsorbed Film Structure. Figure 2 shows 200 by 200 nm images of the adsorbed film structures of the C_{12} alkyl tail surfactants together with their Fourier transforms. The $C_{12}NMe_3Br$ (DTAB) adsorbed film on mica shows parallel stripes meandering across the surface (Figure 2a). The Fourier transform of this image (Figure 2b) shows multiple orders of peaks which yield an average spacing between stripes of 4.8 nm. The uncertainty in this and all lateral spacings reported here is ±0.2 nm. Figure 2 also shows some preferential orientation of the cylinders over this area.

For the larger headgroup of $C_{12}NEt_3Br$, Figure 2c shows the film to consist of aggregates of circular cross section. The difference between the adsorbed layer structure of these two surfactants is evident in the direct and Fourier images. The Fourier transform shows the aggregates have nearest neighbor spacings of 5.0 nm.

The images shown are similar to those reported elsewhere and have been interpreted as full cylinders or full spheres lying on the surface. This is not deduced from AFM images alone: it is consistent with surface force apparatus studies of adsorbed layer thickness for DTAB, cetyltrimethylammonium bromide, and related surfactants.[13,16,17] It is also consistent with adsorption isotherms, which show two steps, and whose ultimate area per molecule is too small to be a monolayer equivalent.[18]

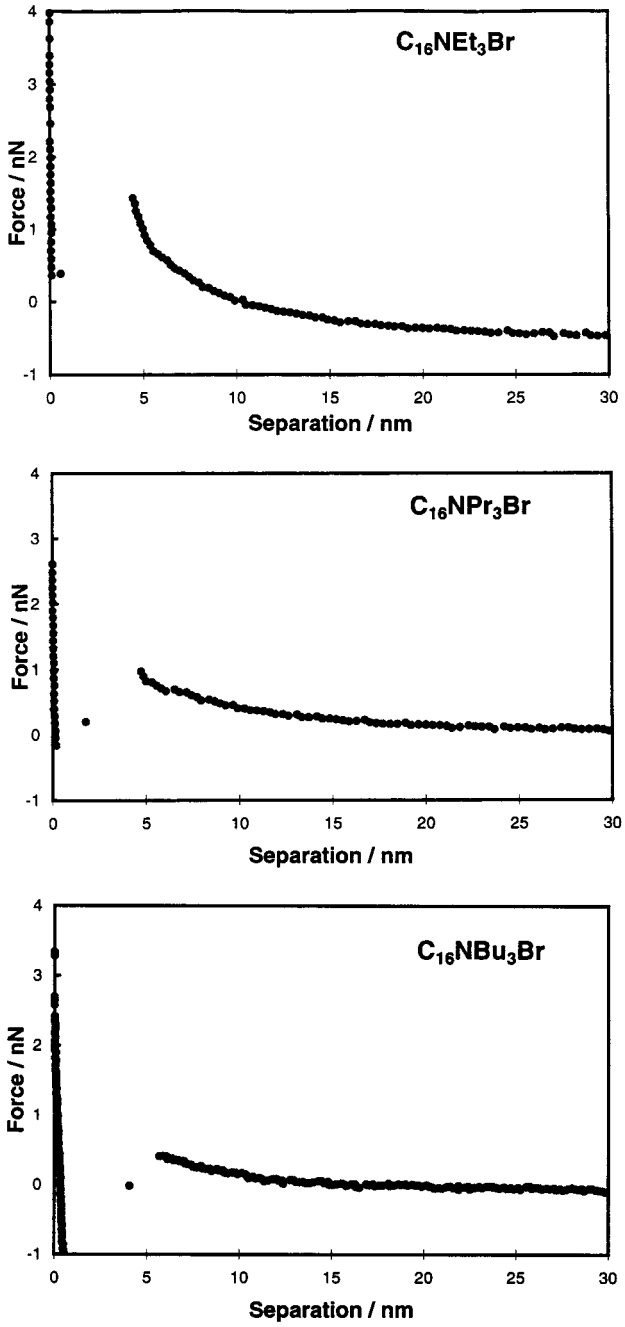

Figure 1. Force versus separation curves for hexadecyltrialkylammonium bromide surfactants adsorbed on mica: (a) 1.4 mM $C_{16}NEt_3Br$; (b) 1.4 mM $C_{16}NPr_3Br$; (c) 0.92 mM $C_{16}NBu_3Br$.

These images are of tip deflection; hence they do not directly measure height. Without knowing the aggregate structure adsorbed on the tip, we cannot directly measure the adsorbed layer thickness. The only inference which can be drawn of the adsorbed film thickness is from the

(16) Kékicheff, P.; Christenson, H. K.; Ninham, B. W. *Colloids Surf.* **1989**, *40*, 31−41.
(17) Pashley, R. M.; McGuiggan, P. M.; Ninham, B. W.; Brady, J.; Evans, D. F. *J. Phys. Chem.* **1986**, *90*, 1637−1642.
(18) Wängnerud, P.; Berling, D.; Olofsson, G. *J. Colloid Interface Sci.* **1995**, *169*, 365−375.

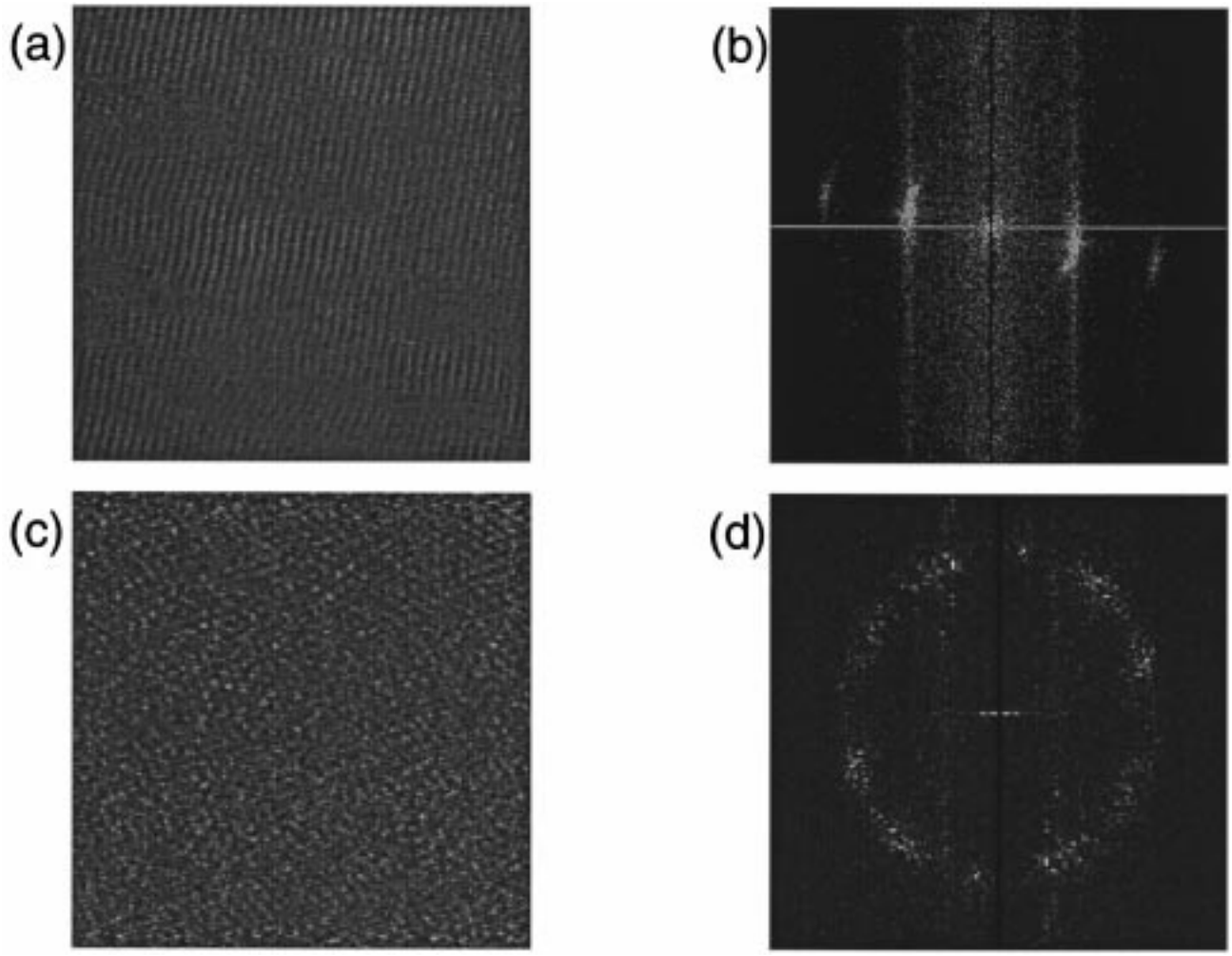

Figure 2. AFM images of dodecyltrialkylammonium surfactants adsorbed on mica. All images are 200 by 200 nm: (a) $C_{12}NMe_3Br$ (DTAB) at 29 mM adsorbed onto mica; (b) its Fourier transform, showing parallel cylindrical micelles of surfactant 4.8 nm apart; (c) $C_{12}NEt_3Br$ at 17 mM; (d) its Fourier transform, showing spherical micelles with nearest neighbor spacing of 5.0 nm.

force curves (Figure 1)—these show films of average thickness 4.2 ± 1.6 nm for all surfactants studied. For comparison, the fully extended length of a C_{12} alkyl chain is about 1.7 nm; twice this length would give a layer thickness which is similar to the measured film thicknesses. We do not know the aggregate structures beyond the breakthrough point; however, previous work on mica suggests that this minimum corresponds to monolayers in hydrophobic contact.[19]

Figure 3a shows the $C_{14}NMe_3Br$ adsorbed film, which consists of meandering full cylinders with a repeat distance of 5.4 nm—this is similar to previous observations of the same system.[6] $C_{14}NEt_3Br$ (Figure 3b), like $C_{12}NEt_3Br$, adsorbs in spherical aggregates with a nearest neighbor spacing of 6.0 nm. Figure 3c shows $C_{14}NPr_3Br$ also forms adsorbed spherical structures. The force profile for $C_{14}NBu_3Br$ was similar to the other surfactants; however no structures could be imaged.

The longer, hexadecyl tail shows somewhat different behavior. Figure 4a shows $C_{16}NEt_3Br$ forms meandering cylinders which are 6.0 nm apart. $C_{16}NPr_3Br$, however, forms short rods (Figure 4b). The differences between these structures are less evident from the Fourier transforms of these two images (shown as insets).

As before, $C_{16}NBu_3Br$ gave a similar force profile, but no structure could be resolved by AFM. Note (Figure 1) the weaker repulsive force with increasing headgroup size; this may be responsible for our inability to image any aggregates. In solution alkyltributylammonium bromides display a lower consolute boundary, indicating an attraction between surfactants, which may also play a role.[15]

The observed geometries for these surfactant aggregates adsorbed on mica are summarized in Table 1. At the concentrations studied (ca. two times the cmc) all of the above surfactants form spherical micelles in solution: yet at the mica−solution interface both spheres and cylinders are observed.

Bulk self-assembly behavior is often rationalized using the surfactant packing parameter, given by[20]

$$g = v/a_0\, l_c$$

Alkyl chain volumes, v, and lengths, l_c, are estimated assuming the chains pack in aggregates at liquid hydrocarbon densities, using the relationships[21,22]

(19) Horn, R. G. *Biochim. Biophys. Acta* **1984**, *778*, 224−228.

(20) Israelachvili, J. N.; Mitchell, D. J.; Ninham, B. W. *J. Chem. Soc., Faraday Trans. 2* **1976**, *72*, 1525−1568.

(21) Gruen, D. W. R *J. Phys. Chem.* **1985**, *89*, 146−153.

(22) Tanford, C. *The Hydrophobic Effect: Formation of Micelles and Biological Membranes*, 2nd ed.; Wiley-Interscience: New York, 1980; p 52.

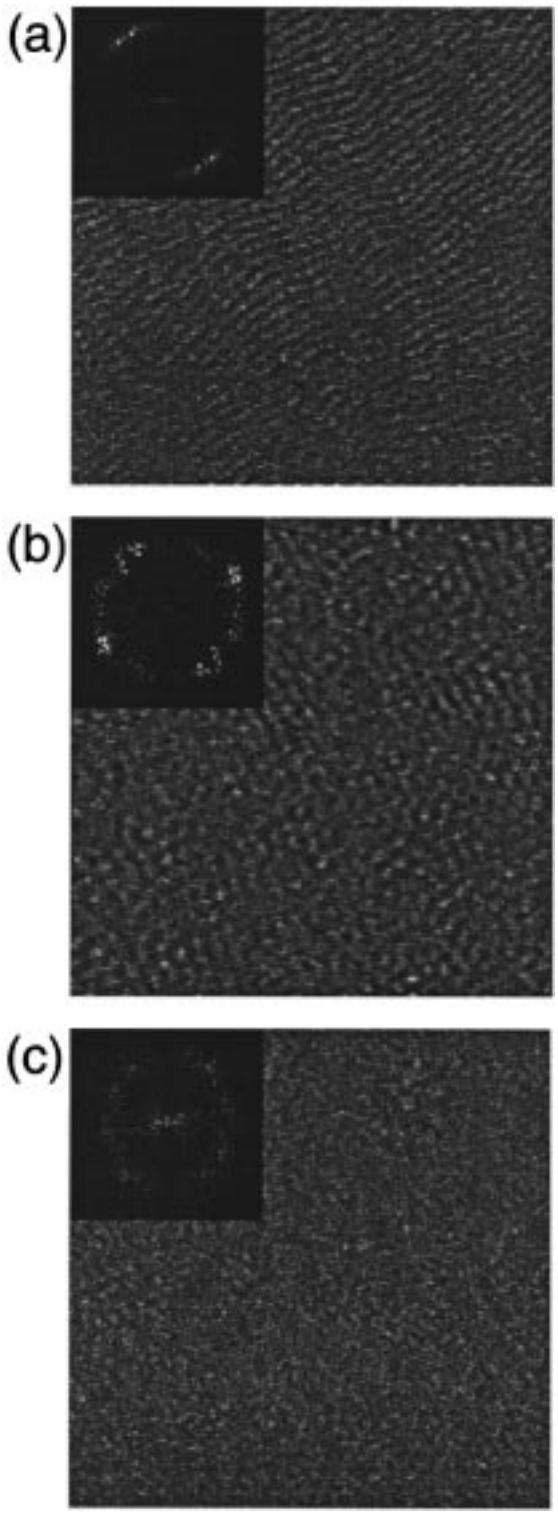

Figure 3. AFM images of tetradecyltrialkylammonium surfactants adsorbed on mica. All images are 200 by 200 nm and Fourier transforms of the images are shown as insets. (a) 7 mM $C_{14}NMe_3Br$ (TTAB) shows meandering cylindrical micelles with a repeat spacing of 5.4 nm; (b) 6.3 mM $C_{14}NEt_3Br$ shows spherical micelles with a nearest neighbor distance of 6.0 nm; (c) 3.0 mM $C_{14}NPr_3Br$ shows globular micelles separated by 5.7 nm.

$$v\ (\text{Å}^3) = 54.30n_{CH_3} + 27.05n_{CH_2}$$

$$l_c\ (\text{Å}) = 2.765 + 1.265n_{CH_2}$$

where a_0 is the area per surfactant headgroup, determined by a balance between surface tension and headgroup repulsion effects. A packing parameter less than 1/3 will yield spherical aggregates, between 1/3 and 1/2 rodlike micelles form, and above 1/2 bilayers form.

All surfactants studied form a spherical micellar phase above the cmc. The area occupied per headgroup is typically 65 Å^2 for trimethyl headgroup surfactants. This is much greater than the steric area due to electrostatic repulsions between charged nitrogen centers. In this case, g is less than 1/3 which indicates spheres and these are observed in solution. With electrolyte addition or with increasing concentration, a sphere-to-rod transition occurs in bulk solution. On adsorption onto mica, however, rods are observed for both C_{12} and C_{14} tails just above the cmc. We postulate that a_0 is reduced on adsorption through the binding of headgroups to negative lattice sites on mica—these have a density of one negative charge per 50 Å^2.[18]

Moving from trimethyl- to tributylammonium headgroups is known to increase a_0 in micelles[23] and at the air−solution interface,[15] as expected from steric considerations. Counterion binding to micelles, as determined from conductivity measurements, is also decreased by increasing the headgroup size. For a given alkyl chain length, increasing the headgroup size decreases the surfactant packing parameter, so favoring spheres over cylinders. This is reflected in each of Figures 2 through 4.

For a given headgroup size, an increasing alkyl chain length might be expected to have no effect on observed aggregate morphologies. Assuming a_0 to be constant, the ratio v/l_c is almost unchanged between C_{12} and C_{16} chains. Experimental studies indicate otherwise: for example, counterion binding increases with chain length. This is one source by which subtle changes in packing parameter might appear.

Certainly the sphere-to-rod transition in micellar solutions occurs at lower electrolyte concentration with longer chains, again indicating an increase in g with chain length. $C_{12}NMe_3Br$ requires 1.8 M NaBr[24] to change from spheres to rods. $C_{14}NMe_3Br$ requires 0.12 M NaBr[25] and $C_{16}NMe_3Br$ requires 0.06 M NaBr.[26] This, too, is reflected in the surface morphologies. Increasing the chain length from C_{14} to C_{16} produces a sphere-to-rod transition for triethylammonium headgroups (Figures 2c, 3b, and 4a), and a sphere-to-short rod transition in the case of the tripropylammonium headgroup (Figures 3c and 4b).

The effect of headgroup size and of alkyl chain length on the phase behavior of various quaternary ammonium surfactants was studied by Blackmore and Tiddy.[14] They showed that the increase in the headgroup size from trimethyl to tributyl results in a reduction in the number of mesophases formed. The phases with lower interfacial curvature, such as lamellar (L_α) and bicontinuous cubic phases (V_1), can no longer form when the headgroup size is increased. This is exemplified by the dodecyl surfactants: $C_{12}NMe_3Br$ forms hexagonal (H_1), V_1, and L_α phases; $C_{12}NEt_3Br$ forms the H_1 phase; $C_{12}NPr_3Br$ forms the H_1 phase; and $C_{12}NBu_3Br$ (along with other tributyl analogues) forms no lyotropic mesophases at all.[14,15]

This phenomenon of a change in aggregation on increasing the tail length by two methylene groups has also been noted in lyotropic phases. An intermediate

(23) Warr, G. G.; Zemb, T. N.; Drifford, M. *J. Phys. Chem.* **1990**, *94*, 4, 3086−3092.
(24) Ozeki, S.; Ikeda, S. *J. Colloid Interface Sci.* **1982**, *87*, 424−435.
(25) Imae, T.; Ikeda, S. *J. Phys. Chem.* **1986**, *90*, 5216−5223.
(26) Imae, T.; Kamiya, R.; Ikeda, S. *J. Colloid. Interface Sci.* **1985**, *108*, 215−225.

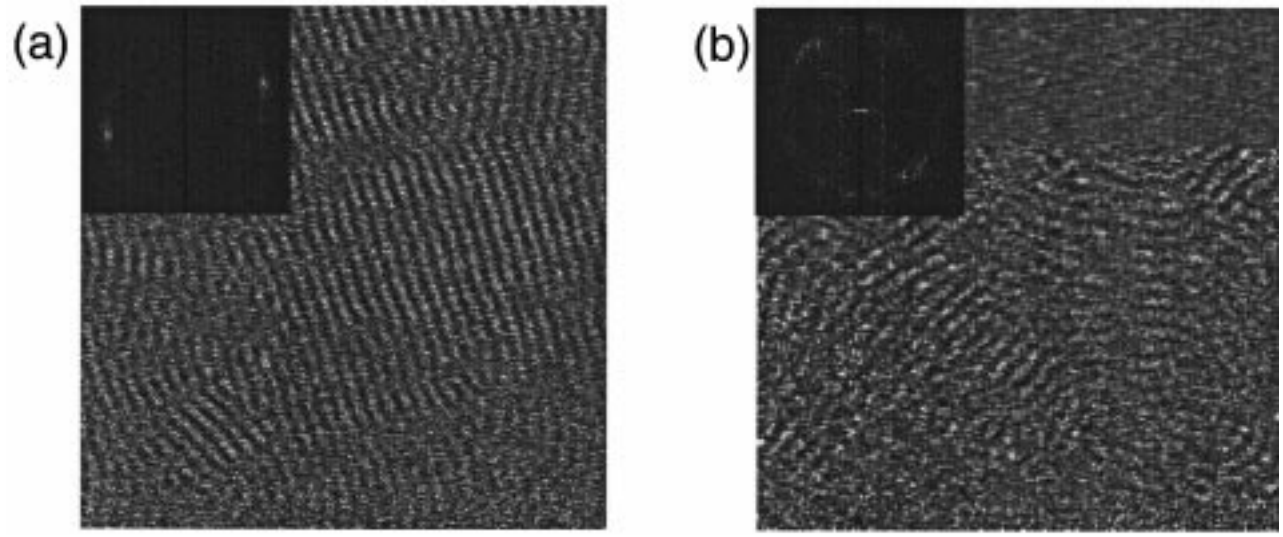

Figure 4. AFM images of hexadecyltrialkylammonium surfactants on mica. Images are 200 by 200 nm, and Fourier transforms of the images are shown as insets. (a) 1.4 mM $C_{16}NEt_3Br$ shows undulating cylindrical micelles 6.0 nm apart; (b) 1.4 mM $C_{16}NPr_3Br$ shows meandering structures which may be short rodlike micelles spaced 6.2 nm apart. Thermal drift has taken this image out of contact in the top third of the scan.

Table 1. Structure of Adsorbed Micelles and Nearest-Neighbor Spacing (nm) for Quaternary Ammonium Surfactants on Mica, Showing the Effect of Different Counterions

alkyl chain length	bromide				chloride	excess salicylate			
	Me_3	Et_3	Pr_3	Bu_3	Me_3	Me_3	Et_3	Pr_3	Bu_3
C_{12}	rods	spheres			spheres	rods	rods		
	4.8 ± 0.2[a]	5.0			5.4	5.1	4.8		
C_{14}	rods	spheres	spheres	soft layer	rods	rods	rods	rods	layer
	5.4	6.0	5.7		5.7	5.4	5.4	5.4	
C_{16}		rods	short rods	soft layer			rods	rods	layer
		6.0	6.2				5.4	5.1	

[a] All reported spacings have an uncertainty of ±0.2 nm.

mesophase forms for the C_{16} and longer alkyl tail lengths but not for shorter chains.[14] Blackmore and Tiddy have postulated that, like block copolymers, C_{16} chains have a sufficient number of conformations that the effective chain length in these micelles is less than the fully extended length, l_c. This has the same effect as increased counterion binding: the packing parameter is increased.

Gemini surfactants of quaternary ammonium salts adsorbed on mica have also recently been shown to follow the same trends of curvature and packing parameter as in bulk solution.[10]

Effect of Counterions. Changing the counterion is known to have a strong effect on the solution behavior of quaternary ammonium surfactants. Critical micelle concentrations,[27] micelle shape,[26,28] and phase equilibria[14] are all influenced by the effect of counterion binding. Direct measurements of ion exchange equilibrium constants give $K^{Cl}_{Br} = 0.3$[29,30] and $K^{salicylate}_{Br} = 48$ (for TTAB).[31] All experimental studies agree on the binding order

$$Cl^- < Br^- < \text{salicylate}$$

and on the exceptionally strong binding of salicylate. Recent studies indicate that salicylate binds less strongly to surfactants with larger headgroups, but always much more strongly than bromide.[32]

Adsorbed films of alkyltrimethylammonium chlorides of various chain lengths adsorbed onto mica are shown in Figure 5. $C_{12}NMe_3Cl$ forms spherical aggregates[33] and $C_{14}NMe_3Cl$ forms cylindrical aggregates. Their spacings are summarized in Table 1. The aggregation patterns are different from the bromide analogues, and this is paralleled in their solution structures and phase equilibria.

In bulk solution, chloride salts show differences in behavior due to their weaker ion binding compared to bromide. For example, the sphere-to-rod transition in $C_{16}NMe_3Cl$ requires 1.2 M NaCl,[34] which is 10−20 times higher than that for bromide. Similar effects are observed in phase equilibria: both $C_{12}NMe_3Cl$ and $C_{14}NMe_3Cl$ have close-packed micellar (I_1) cubic phases, indicating the persistence of spheres to very high surfactant concentrations. These phases are absent in the corresponding bromides: indeed, $C_{14}NMe_3Br$ forms a rodlike nematic phase near room temperature.[35]

Addition of the salicylate ion produced two effects: an

(27) (a) Anacker, E. W.; Underwood, A. L. *J. Phys. Chem.* **1981**, *85*, 2463−2466. (b) Underwood, A. L.; Anacker, E. W. *J. Phys. Chem.* **1984**, *88*, 2390−2393. (c) Underwood, A. L.; Anacker, E. W. *J. Colloid Interface Sci.* **1984**, *100*, 128−135. (d) Underwood, A. L.; Anacker, E. W. *J. Colloid Interface Sci.* **1985**, *106*, 86−93.

(28) Quirion, F.; Magid, L. J. *J. Phys. Chem.* **1986**, *90*, 5435−5441.

(29) Morgan, J. D.; Napper, D. H.; Warr, G. G.; Nicol, S. K. *Langmuir* **1994**, *10*, 797−801.

(30) Kellaway, L.; Warr, G. G. *J. Colloid Interface Sci.* **1997**, *193*, 312−314.

(31) Thalody, B.; Warr, G. G. *J. Colloid Interface Sci.* **1995**, *175*, 297−303.

(32) Cassidy, M. A.; Warr, G. G. Manuscript in preparation.

(33) This is in contrast to previous results for $C_{12}NMe_3Cl$ which showed it formed cylindrical micelles on mica (see: Manne, S. *Prog. Colloid Polym. Sci.* **1997**, *103*, 226−233). In our case, the initial images of $C_{12}NMe_3Cl$ had a striped appearance, but there was an evolution to the spheres shown here possibly due to ion exchange effects.

(34) Imae, T.; Ikeda, S. *Colloid Polym. Sci.* **1987**, *265*, 1090−1098.

(35) Boden, N. In *Micelles, Membranes, Microemulsions, and Monolayers*; Gelbart, W. M., Ben-Shaul, A., Roux, D., Eds.; Springer: Berlin, 1994; pp 153−211.

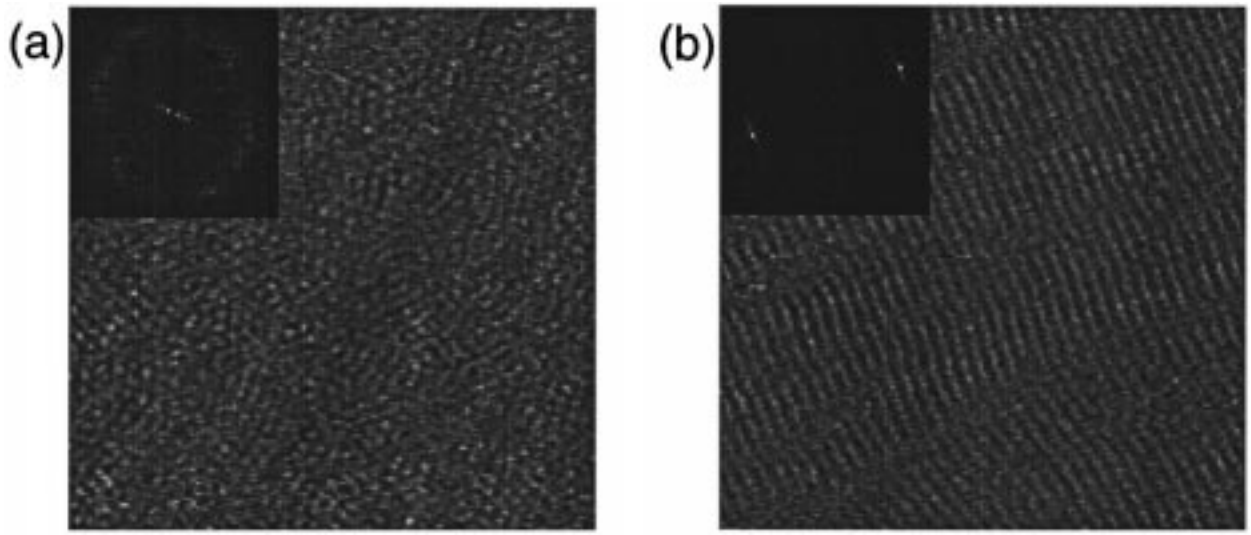

Figure 5. AFM images of chloride salts of alkyltrimethylammonium surfactants on mica. Images are 200 by 200 nm and Fourier transforms of the images are shown as insets. (a) 38 mM $C_{12}NMe_3Cl$ shows spherical micelles spaced 5.4 nm apart; (b) 9.1 mM $C_{14}NMe_3Cl$ shows parallel cylindrical micelles 5.7 nm apart.

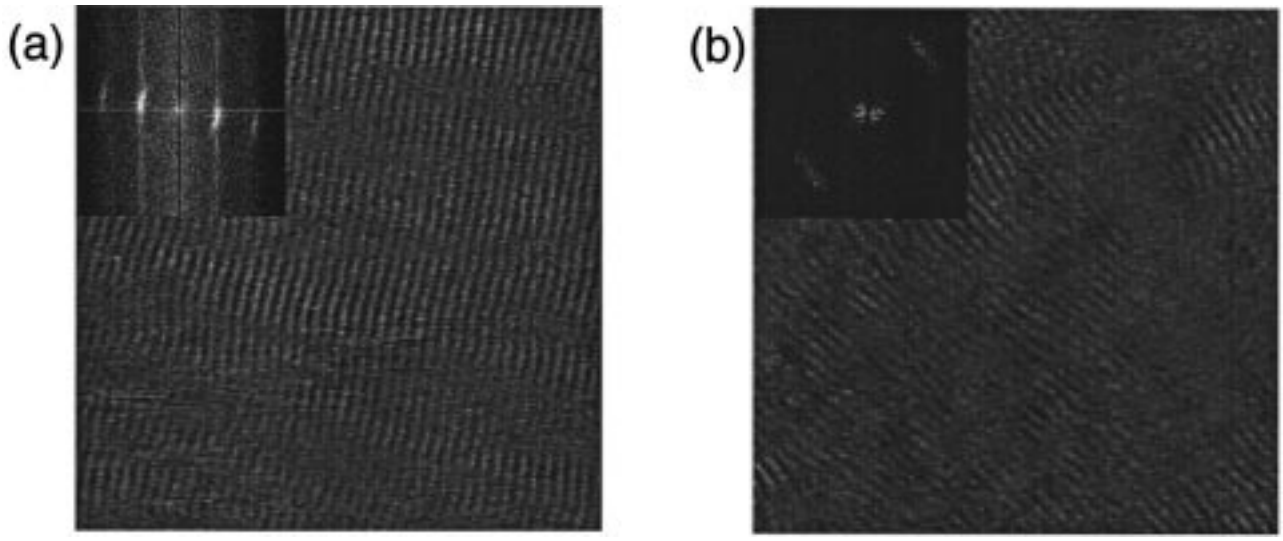

Figure 6. AFM images of dodecyltrialkylammonium surfactants on mica with added salicylate. Images are 200 by 200 nm and Fourier transforms of the images are shown as insets. (a) 29 mM $C_{12}NMe_3Br$ shows cylindrical micelles 5.1 nm apart; (b) 17 mM $C_{12}NEt_3Br$ shows cylindrical micelles 4.8 nm apart.

increase in the stability of imaging the adsorbed layer and a change in adsorbate structure where possible. In all cases imaging using a double layer repulsive force was facilitated by salicylate ions. The stability of the adsorbed film was increased such that scans were highly reproducible: adsorbed structures were stable to changes in scan rate, scan direction, and scan size. Virtually no drift in cantilever position perpendicular to the solid plane throughout a scan occurred.

The second effect was the alteration of the adsorbed aggregate structure by the counterion. All surfactant solutions showed meandering, cylindrical aggregates after the addition of salicylate solution with the exception of the tributyl headgroups where, again, no lateral structure could be observed. As can be seen in Figures 6, 7, and 8, salicylate ions changed the adsorbed aggregates from spheres for $C_{12}NEt_3Br$ and $C_{14}NEt_3Br$ and from short rods for $C_{16}NPr_3Br$ to meandering cylinders. Other adsorbed cylinders retained their morphology (Figure 8). The observed changes in aggregate geometries on the addition of sodium salicylate are summarized in Table 1. These structures parallel the bulk properties of these surfactants with salicylate as the counterion. Micelles with salicylate counterions are long, entangled, and wormlike.[36] The phase diagrams of C_{14} trimethyl, triethyl, and tripropyl surfactants with salicylate all contain the hexagonal phase as the first lyotropic mesophase, but these form at lower concentrations than that with bromide as the counterion.[32]

To understand the effect of salicylate on adsorbed film structure at a semiquantitative level, we consider only the steric contribution to the area occupied by the headgroup of cationic surfactants. In the limit of strong binding of an ion which does not itself contribute to the packing parameter, the structure formed will depend on contact between headgroups. By analogy with the surfactant packing parameter, the steric packing parameter is defined as

$$g_{st} = v/a_{st}\, l_c$$

where a_{st} is the area per headgroup, excluding electrostatic effects. We can calculate the steric packing parameter for

(36) Imae, T.; Kohsaka, T. *J. Phys. Chem.* **1992**, *96*, 10030−10035.

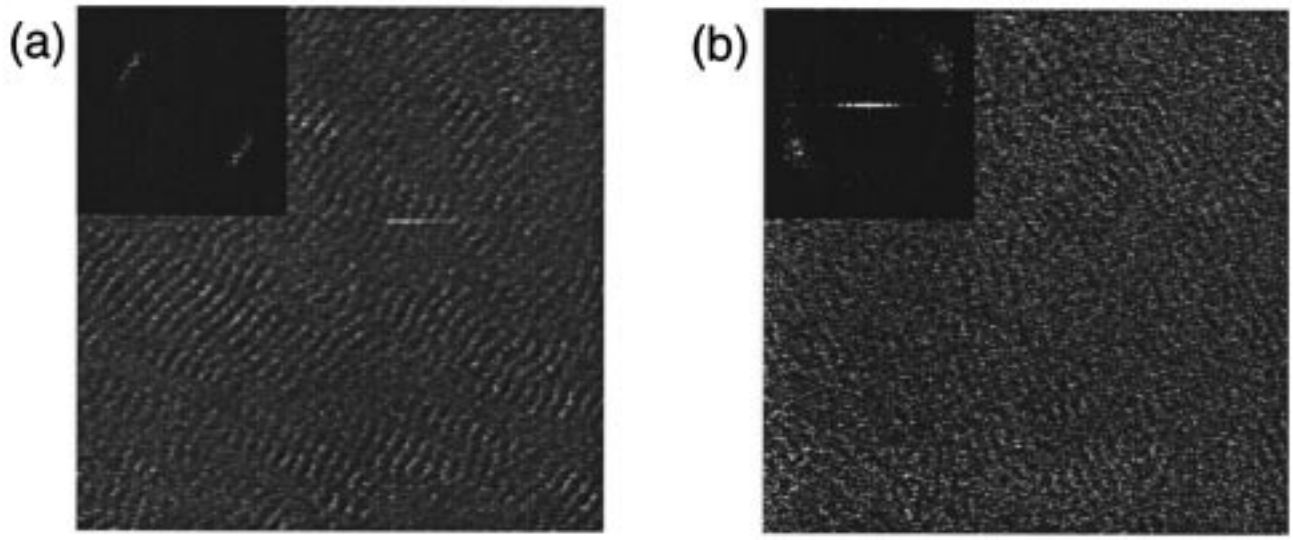

Figure 7. AFM images of tetradecyltrialkylammonium surfactants on mica with excess salicylate. Images are 200 by 200 nm and Fourier transforms of the images are shown as insets. (a) 6.3 mM $C_{14}NEt_3Br$ shows cylindrical micelles 5.4 nm apart; (b) 3.0 mM $C_{14}NPr_3Br$ shows cylindrical micelles 5.4 nm apart.

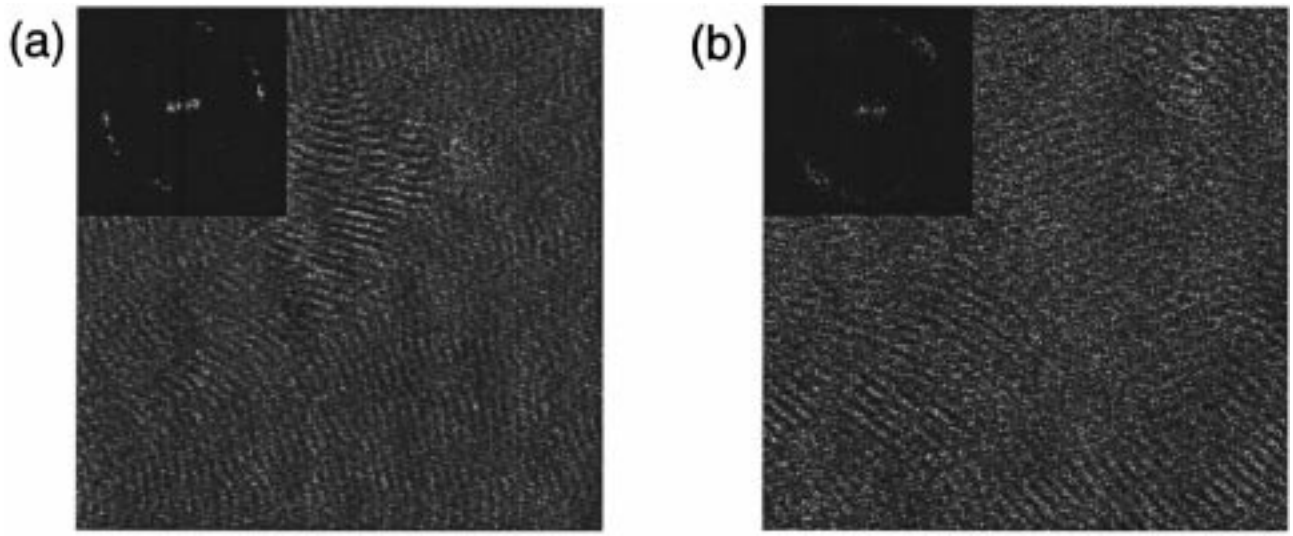

Figure 8. AFM images of hexadecyltrialkylammonium surfactants on mica with added salicylate. Images are 200 by 200 nm and Fourier transforms of the images are shown as insets. (a) 1.4 mM $C_{16}NEt_3Br$ shows cylindrical micelles 5.4 nm apart; (b) 1.4 mM $C_{16}NPr_3Br$ shows cylindrical micelles 5.1 nm apart.

Table 2. Steric Packing Parameter, g_{st}

	headgroup type			
alkyl chain length	$-NMe_3$	$-NEt_3$	$-NPr_3$	$-NBu_3$
C_{12}	0.65	0.43	0.39	0.26
C_{14}	0.66	0.43	0.39	0.26
C_{16}	0.66	0.43	0.39	0.26

the trialkylammonium surfactants in this work from measurements of CPK molecular models. These give the minimum areas for trimethyl-, triethyl-, tripropyl-, and tributylammonium headgroups; the values used were trimethyl 32 Å^2, triethyl 49 Å^2, tripropyl 54 Å^2, and tributyl 80 Å^2.

The steric packing parameter thus gives an upper bound to the permitted packing parameter. Calculated steric packing parameters are shown in Table 2. Thus the minimum curvature aggregates allowed by steric constraints are bilayers for trimethylammonium headgroups, cylinders for triethyl and tripropyl headgroups, and only spheres for tributyl. The fact that we do not observe a bilayer with the salicylate ion may be due to intercalation effects which increase v or to other specific binding effects.[36,37] The correlation with bulk phase equilibria remains; none of these quaternary ammonium bromide surfactants form a lamellar phase in the presence of equimolar salicylate.

Conclusions

The aggregation patterns of cationic surfactants in adsorbed films on mica parallel those observed in bulk for both micellar solutions and more concentrated phases. Although shifted toward lower curvature aggregates, systematic structural changes within the molecules lead to changes in the adsorbed layer structure on mica which agree with expectations from the surfactant packing parameter. Even subtle effects such as chain length variation produce similar effects in bulk as at this interface. We expect that the same would be observed in an adsorbed film on any other surface with the same kind of adsorption mechanism.

(37) Cassidy, M. A.; Warr, G. G. *J. Phys. Chem.* **1996**, *100*, 3237−3240.

This contrasts with the adsorption of surfactants on graphite, where the adsorbed layer structures are determined by strong adsorbate/adsorbent interactions. On mica the interactions between the adsorbed molecules—i.e., self-assembly—are equally important and give rise to a much greater range of adsorbed film morphologies.

Acknowledgment. This work was funded by the Australian Research Council and the MRSEC program of the National Science Foundation (DMR-940032) and was made possible by the University of Sydney Special Studies Program. H.N.P. acknowledges the receipt of an Australian Postgraduate Award.

LA981612O